Fan Mo*, Anastasia Borovykh, Mohammad Malekzadeh, Hamed Haddadi, and Soteris Demetriou

Quantifying and Localizing Private Information Leakage from **Neural Network Gradients**

Abstract: Empirical attacks on collaborative learning show that the gradients of deep neural networks can not only disclose private latent attributes of the training data but also be used to reconstruct the original data. While prior works tried to quantify the privacy risk stemming from gradients, these measures do not establish a theoretically grounded understanding of gradient leakages, do not generalize across attackers, and can fail to fully explain what is observed through empirical attacks in practice. In this paper, we introduce theoretically-motivated measures to quantify information leakages in both attack-dependent and attackindependent manners. Specifically, we present an adaptation of the V-information, which generalizes the empirical attack success rate and allows quantifying the amount of information that can leak from any chosen family of attack models. We then propose attackindependent measures, that only require the shared gradients, for quantifying both original and latent information leakages. Our empirical results, on six datasets and four popular models, reveal that gradients of the first layers contain the highest amount of original information, while the (fully-connected) classifier layers placed after the (convolutional) feature extractor layers contain the highest latent information. Further, we show how techniques such as gradient aggregation during training can mitigate information leakages. Our work paves the way for better defenses such as layer-based protection or strong aggregation.

Keywords: Information Privacy, Deep Neural Networks.

Hamed Haddadi: Imperial College London, E-mail:

h.haddadi@imperial.ac.uk

Soteris Demetriou: Imperial College London, E-mail: s.demetriou@imperial.ac.uk

1 Introduction

The training process of deep neural networks (DNNs) is increasingly outsourced to the individuals' devices. a la collaborative/federated learning [1, 2], due to distributed computational powers and data privacy issues. Instead of sharing private data, participants share the DNN model updated on their data. The updated model is thus composed of the *original model* and *gradients*. It is well-known that one can still extract private information from these gradients using attacks such as input data reconstruction [3, 4] aiming to restore the original data (e.g., a face image), and attribute inference [5] aiming to infer a *latent* attribute of the data (e.g., the race or age of a person). Attacks on a DNN's gradients are shown to be effective in practice [6–10], but more fundamentally it is not yet clear what the characteristics are of models that can leak sensitive information and to what degree different types of private information are stored in the gradients. Existing research considers information leakage to be a result of insufficient generalization performance or unintended memorization [11–13], but the specifics as to the relation of leakages to model architecture, training method, and dataset are still seen as open problems.

The most common method for measuring the risk of sharing gradients is the attack success rate: the accuracy of a specific attack in extracting a specific piece of information. However, this technique lacks a theoretical foundation and enables reasoning about the leakages only for a specific attack type. Previous works tried to better understand the information stored in DNNs by analyzing the information flow through the layers of a DNN e.g., by measuring mutual information (MI) [14–17] or by visualizing the intermediate representation (i.e., a layer's output) [18–20]. However, these methods mostly analyze the forward propagation at the inference stage and do not explain information leakages in terms of gradients produced in the backward propagation, which is the pivotal part of the DNN training stage. Furthermore, as we will demonstrate later in this paper, while MI and visualization (i.e., t-SNE projection) methods characterize initial layers to be the most prone to leakage, our experimental results show that such a conclusion is not

^{*}Corresponding Author: Fan Mo: Imperial College London, E-mail: f.mo18@imperial.ac.uk

Anastasia Borovykh: Imperial College London, E-mail: a.borovykh@imperial.ac.uk

Mohammad Malekzadeh: Imperial College London, E-mail: m.malekzadeh@imperial.ac.uk

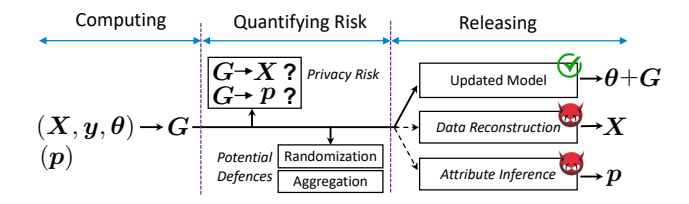


Fig. 1. Overview: gradients G, w.r.t. the model's parameters θ , is locally computed on private data X and label y. Sharing G allows collaboratively optimizing θ , but it also results in privacy risks of disclosing either the original data or a private attribute p. We show how to quantify private information leakage from G and discuss the effect of potential defences.

always consistent with what is empirically observed in successful attacks.

In this work, we establish methodologies for quantifying and localizing information leakages from gradients in both attack-dependent and attack-independent manners. Having the right tools for understanding in what amount and where sensitive information is stored in the models' gradients can guide the design of better privacy protection mechanisms. As shown in s/ure 1, our methodologies can serve as the privacy risk quantification tools when releasing gradients. For example, participants could share only a fraction of their gradients [21, 22] or a part of the gradients could be processed in devices' Trusted Execution Environments (TEE) [23–25].

We investigate leakages on two main types of information: i) original information, the observed data in clients' training datasets, and ii) latent information, attributes or properties of the observed data, in this way covering most existing critical attacks on gradients. We first define an umbrella framework that encompasses the attack success rate but allows to reason about leakages for a family of attackers having certain model characteristics by adapting the information-theoretical \mathcal{V} information [26]. In order to further understand what characteristics of the trained model make it prone to gradient leakages, we present two quantities that capture gradient changes w.r.t. original and latent information based on sensitivity and subspace distances, respectively. As their computation relies only on the trained model itself they can help understand leakages independently of the attack model.

Contributions: i) We define a theoretical foundation underlying attack success rates. This results in a unifying framework for attack success rates that allows us to differentiate between the computational power of the chosen attack family and its relationship to how much

and what kind of leakage can occur. In this way, our work better explains the relationship between empirical attack results and theoretical information analysis; ii) We localize private information in the gradients produced in the backward propagation. While the first layers of a model contain the most original information, our characterization is the first to reveal that fully-connected layers of the classifier in most standard networks (i.e., convolutional neural networks) contain the highest latent information; iii) We show that information leakages are highly predictable using gradient change measures. The definition of such measures give additional tools for understanding in an attackindependent manner why gradient leakages happen, how this depends on the underlying training mechanisms and datasets, and how to protect against it; iv) We extensively analyze the effect of training hyperparameters and different datasets. We show that the epoch does not significantly influence information leakages, while gradient aggregation (e.g., $30\sim50$ times of non-target information) could significantly reduce information leakages. Our analysis also indicates that DP noise addition with different layers results in completely different effectiveness in obfuscating either original or latent information.¹

2 Problem Formulation

Notation. We use lower-case italic, e.g., x, for deterministic scalars, lower-case bold italic, e.g., x, for deterministic vectors, and upper-case bold italic, e.g., X, for deterministic matrices. Also, roman-type upper-case, e.g., X, and lower-case, e.g., x, denote random variables (of any dimensions) and their instances, respectively. Table 1 summarises frequently used notations in this paper.

Terminology. In this work we distinguish between two types of private information i) original information, *i.e.*, the explicit data considered to contain private information about its owner, such as a complete private image used for model training, and ii) latent information, *i.e.*, implicit data contained in or related to the original information, such as attributes/properties or parts of the image. The starting point of this distinction between two types of information is inspired by corresponding attacks, *i.e.*, data reconstruction attacks and attribute/property information attacks, as they exist in

¹ Codes are anonymously available through the following link: https://bit.ly/3fn7nzx

Table 1. Frequently used notation.

| Symbol | Description |
|---|---|
| \overline{X} , \overline{X} and \overline{x} | Original information * |
| T_l , \mathbf{T}_l and \mathbf{t}_1 | Intermediate representation of layer $l\ *$ |
| G_l , \mathbf{G}_l and \mathbf{g}_l | Gradient of layer l ** |
| p , \mathbf{P} and \mathbf{p} | Latent attribute or input data *** |
| $\overline{{ m J}_l^{(G)}(X)}$ | Input-gradient Jacobian of layer l^{th} |
| I(X; G) | Mutual information between $\mathbf X$ and $\mathbf G$ |
| $\mathcal{R}_l^{(X)}$, $\mathcal{R}_l^{(p)}$ | Original and latent information risk of layer $l^{ m th}$ |
| $\mathcal{V}_{\mathcal{A}}$ | Predictive family of Adversary ${\cal A}$ |
| $\mathbb{G}_{l}^{(0)}$, $\mathbb{G}_{l}^{(1)}$ | Linear subspaces of layer l^{th} 's gradients without |
| | and with an attribute |
| $f_{\mathcal{A}}[\mathrm{g}_l](\mathrm{x})$ | Distribution evaluated at ${f x}$ based on ${f g}_l$ |
| $\hat{I}_{\mathcal{V}_{\mathcal{A}}}(\mathrm{G}_l 	o \mathrm{X})$ | Empirical ${\mathcal V}$ -information from ${ m G}_l$ to ${ m X}$ |
| $d_{\mathbf{Gr}}(\mathbb{G}_l^{(0)},\mathbb{G}_l^{(1)})$ | Grassmann distance between subspaces |

^{*} deterministic matrix, random variable and instance;

different conditions and have different attack strategies. We will often use the following notation for them: let \boldsymbol{X} denote one client's (deterministic) private training data, and \boldsymbol{p} denote one type of latent information of the data. The original information leakage risk is then measured by how much information about X an adversary can extract, and the latent information leakage risk is measured by how much information about P an adversary can extract from the gradients. We explain these gradient-based attacks in detail in the following section.

3 Gradient-based attacks

3.1 Gradient Sharing

In collaborative/federated learning, multiple clients collaboratively train a model while keeping the training data at the client's side [1, 27]. The gradient updated over one batch of a client's data (denoted as G^1), is computed by $\frac{\partial \ell(X,y,\theta^0)}{\partial \theta^0}$, where X and y denote this training data and corresponding labels, θ^0 refers to the original model parameters, and $\ell(\cdot)$ refers to the loss function. This G^0 consists of all model layers' gradients which in typical collaborative learning settings is the minimum that must be shared to another participant (e.g., server). In more communication-constrained scenarios, it is preferable to consecutively update the model on more batches of local data [1] before shar-

ing. After the t-th batch, the updated weights are given by $\theta^t = \theta^0 + \sum_{i=1}^t G^i$, where G^i is the gradients of i batch computed based on θ^i . This local training can last for several epochs. For training on one client, we later do not distinguish one or multiple batches and refer $\sum_{i=1}^t G^i$ as G and θ^t as θ for simplicity.

Although commonly a client shares the last snapshot of the updated model that consists of the original model and computed gradients $(i.e., \theta + G)$, this practically amounts to sharing G since all participants know θ . Private information can then be compromised by the attacker as this G could contain private information explicitly or implicitly. The gradient sharing can be among clients and the central server in any direction depending on the specific settings [3, 24, 27]. While gradients shared from the clients are more relevant to that specific clients, the gradients shared from the center usually are aggregated across the clients, meaning that disclosing private information of one particular client from that 'central' gradients becomes harder.

3.2 Attack types

The main intention of sharing gradients is to learn a model without revealing clients' private data. However, as mentioned before, from the gradients computed over training data this private information can still be extracted. We begin with a brief overview of the specific attack models used to extract i) original information and ii) latent information.

Original information attack. In order to extract the exact i) original information, the data reconstruction attack (DRA) [3, 4, 8] works by randomly initializing dummy data and feeding it into the model to get dummy gradients. Then, the dummy data is optimized such that the dummy gradients get close to the real gradients. More specifically, the DRA tries to minimize the following objective by updating both dummy input X' and dummy label y',

$$\operatorname{argmin}_{\mathbf{X}',\mathbf{y}'}||\mathbf{G}' - \mathbf{G}||_p, \tag{1}$$

where G' and G denote the dummy and real gradient, respectively and $||\cdot||_p$ can be any suitably chosen norm. We remark that X' and y' can be one individual data point or a batch of data points. Once this objective is sufficiently small, the dummy input data will be close to the real private information. For a batch size B > 1, the optimizer can have B! different permutations, so that choosing the right gradient descent direction is compli-

^{**} deterministic vector, random variable and instance;

^{***} deterministic scalar, random variable and instance.

cated - as a solution a single training sample can be updated in each optimization step [3].

DRAs can reach high accuracy (e.g., to a pixel-wise level for images) as shown in experiments [3, 8]. However, it may fail when gradients have sufficient aggregation (e.g., a large batch size) because the optimization becomes hard to solve (i.e., more variables to optimize over than we have constraints) when the gradients of multiple images are mixed together [3]. The impact of aggregation will the explored more deeply in the later sections.

Latent information attack. With a stronger aggregation, extracting 'high-level' information (i.e., information that is more abstract and with lower entropy) may be a more feasible choice. That is, instead of disclosing the exact data point, one attacker aims to disclose latent information such as attributes of the data point. The attribute inference attack (AIA) [5, 6, 28] focuses on extracting private attributes of the client's data. One way of conducting the attack is to collect multiple snapshots of the model and feed them with the attacker's own data with/without a certain target attribute to obtain corresponding gradients of the data. The gradients and their attribute labels are used to train a binary classifier that can distinguish whether an obtained set of gradients was computed on clients' data with a target attribute or without it. Specifically, the attack works as follows. We assume the adversary has access to a batch of data with an attribute and without an attribute. We assume that the adversary was able to collect a set of gradients $\{G_1^0, ..., G_T^0\}$ and $\{G_1^1, ..., G_T^1\}$ where T refers to the iterations in which the adversary managed to get the model parameters and consequently pass a subset of data with and without the property through the model to compute the gradients. Having obtained these two sets of gradients the model then trains a binary classifier on the model so that given a new gradient sample one can classify it as coming from a dataset where the (majority of) data samples are with or without the chosen attribute. The binary classifier can use a loss function such as the cross-entropy loss. The success of such an attack thus relies on how well the classifier can distinguish the samples from the gradients with the attributes from those without. We note that there is another famous attack called membership inference attack (MIA), exploring the existence of a particular client's data in the training dataset [6, 29]. The data point's existence can be regarded as one kind of 'high-level' latent information. Indeed, membership decides whether one data exists or not, while the original information tries to reconstruct the data exactly. Furthermore, the membership information could be regarded as one "attribute" of the input, because according to Yeom et al. [11]'s research, membership leakage risks are deeply correlated to and within a constant factor of the attribute leakage risks

The relation between original and latent information. One may observe that P can be extracted from X, i.e., once the original data is recovered it is possible to identify the attributes presented in the data. However, this does not imply that the two types of information are equivalent in terms of their cause and localization. Specifically, while the ability to extract latent information from original information holds true, the reverse does not. Knowing the attribute present in a subset of the data does not always allow to recover each individual data point. This is in turn related to the fact that aggregation, i.e., the computation/aggregation of the gradients over larger batches of data, can protect against original information leakages, but still allows to extract whether the majority of the data had a certain attribute. This is somewhat related to observation in previous research e.g., [30, 31] that when recovering original data a unique global minimizer of (1) does not always exist or may be computationally very hard to find. Furthermore, the computational power of the adversary is crucial in determining what kind of information it is able to extract. In latter layers, a model has already performed more modifications on the data. These modifications may result in an attacker with smaller computational power still being able to extract this latent information. This does not imply that less latent information is present in earlier layers (in other words, the data processing inequality we will explain in Section 4.1 still holds for latent information), however earlier layers will require the attacker to perform more heavy computations on this data to infer the attributes. Therefore we conclude the following: i) when and where information is stored is different for original and latent information, ii) the computational power of the adversary determines what kind of information is possible to extract.

3.3 Gradient Computation

Forward and backward propagation. In order to better understand how models leak sensitive information through gradients we revisit how gradients are computed as a function of the input. Let $X = [x_1, \ldots, x_K]$ be one batch of data consisting of K samples from client c's training dataset \mathcal{D}^c , and let $Y = [y_1, \ldots, y_K]$ be the corresponding ground truth (e.g., labels) for a classifica-

tion task). The complete training dataset of all C clients is denoted by the set $\mathcal{D} = \{\mathcal{D}^1, ..., \mathcal{D}^C\}$. For a DNN model with L layers, we denote layer l^{th} 's parameters with \mathbf{W}_l and \mathbf{b}_l ; the weights and biases, respectively. In the forward propagation from layer l^{st} to L^{th} , the layer l^{st} computes

$$A_l = [a_{l,1}, \dots, a_{l,K}] = W_l T_{l-1} + b_l \mathbf{1}^\mathsf{T},$$
 (2)

where $\boldsymbol{W}_l \in \mathbb{R}^{N_l \times N_{l-1}}$, $\boldsymbol{T}_{l-1} = [\boldsymbol{t}_{l-1,1}, \ldots, \boldsymbol{t}_{l-1,K}] \in \mathbb{R}^{N_{l-1} \times K}$, $\boldsymbol{b}_l \in \mathbb{R}^{N_l}$, $\boldsymbol{1} \in \{1\}^K$. N_l denotes the size (i.e., the number of neurons) of the layer l^{th} , and \boldsymbol{T}_{l-1} shows the intermediate representation that is the output of the (previous) layer $l-1^{\text{th}}$, and $\boldsymbol{t}_{l-1,k}$ corresponds to one sample k's outputs. Then, the layer l^{th} 's output is $\boldsymbol{T}_l = [\sigma(\boldsymbol{a}_{l,1}), \ldots, \sigma(\boldsymbol{a}_{l,K})] \in \mathbb{R}^{N_l \times K}$, denoted as $\sigma(\boldsymbol{A}_l)$ for simplicity, where $\sigma(\cdot)$ is the chosen activation function. Note that $\boldsymbol{T}_0 = \boldsymbol{X}$ and $\boldsymbol{T}_L = \hat{\boldsymbol{Y}}$ the prediction on ground truth.

In the backward propagation, the loss ℓ between $\hat{\boldsymbol{Y}}$ and \boldsymbol{Y} propagates from the layer L^{th} to 1^{st} . For layer l^{th} , the gradient vector \boldsymbol{G}_l consists of the gradients of the weights and biases $\{\boldsymbol{G}_l^{(w)}, \boldsymbol{G}_l^{(b)}\}$, which are computed using the chain rule:

$$G_l^{(w)} = \frac{\partial \ell}{\partial W_l} = \frac{\partial \ell}{\partial A_l} \frac{\partial A_l}{\partial W_l} = \frac{\partial \ell}{\partial A_l} T_{l-1}^{\mathsf{T}}$$
(3)

$$G_l^{(b)} = \frac{\partial \ell}{\partial b_l} = \frac{\partial \ell}{\partial A_l} \frac{\partial A_l}{\partial b_l} = \frac{\partial \ell}{\partial A_l} \mathbf{1}$$
 (4)

where $G_l^{(w)} \in \mathbb{R}^{N_l \times N_{l-1}}$ and $G_l^{(b)} \in \mathbb{R}^{N_l}$ and have the same size with W_l and biases b_l respectively.

The set of all layers' $G^{(w)}$ and $G^{(b)}$ in Equation (3) and (4) is the minimum unit to update in a model sharing scenario, for example, corresponding to the generic Federated stochastic gradient descent method (FedSGD) [1]. $G^{(w)}$ and $G^{(b)}$ are also targeted by adversaries to extract private information of X or its sub-information e.g., p. In another method called Federated Averaging (FedAvg) [1], before updating, more batches of data are fed for training, and the gradients of multiple batches are aggregated together element-wisely by

$$\sum_{\boldsymbol{X}_{i} \in \mathcal{D}^{c}} \{\boldsymbol{G}_{l}^{(w)}\}_{\boldsymbol{X}_{i}}; \sum_{\boldsymbol{X}_{i} \in \mathcal{D}^{c}} \{\boldsymbol{G}_{l}^{(b)}\}_{\boldsymbol{X}_{i}}$$
 (5)

General analysis on privacy risks of gradients. Here we directly analyze how G leaks information of X or p based on Equation (3), (4), and (5). Three observations on information leakage from DNN parameters (*i.e.*, gradients) are: 1) One can obtain the layer l^{th} 's input (T_{l-1}) based on this layer's gradient updates. Because the first layer's input (*i.e.*, T_0) is X, the input

is highly likely to be leaked. This has been discussed in previous research [32], which also could be the reason for the success of DRAs. Thus, the first layers may contribute more in the privacy risk related to DRAs.

- 2) Batch-based training (i.e., batch size > 1) reduces the potential leakage on one specific data sample $x_i, i \in 1, ..., K$, because gradients are computed over all samples in one batch (see Equation (3) and (4)). This has also been confirmed in DRAs [3]. Besides, further aggregation, i.e., the summation of gradients over multiple batches, also reduces the potential leakage (see Equation (5)).
- 3) The term $\frac{\partial \ell}{\partial A_l} = \frac{\partial \ell}{\partial T_l} \odot \sigma'(a_l) = W_{l+1}^\mathsf{T} \frac{\partial \ell}{\partial A_{l+1}} \odot \sigma'(A_l)$ (note that \odot is the Hadamard product), indicating that the gradient can potentially contain information of A_l , W_{l+1} , b_{l+1} , and parameters of following layers (*i.e.*, A_{l+1} , ..., A_L). However, as we will explain in Section 4.1 the Data Processing Inequality (DPI) from layer 1st to L^{th} indicates that T_{l+1} (or a_{l+1} here) cannot contain more information on X than T_l (or a_l) [14–16]. Therefore, to determine the location of the largest amount of information in G is not as straightforward as analyzing information flow in T.

4 Information theory for gradient leakages

Gradient sharing can be seen as a communication channel. At the sender side (*i.e.*, client), we have an encoder that transforms original data into the gradients, and at the receiver side (*i.e.*, server), we have a decoder that transforms the received gradients into a collaboratively trained model. In this view, a wire-tapper (*i.e.*, attacker) wants to learn as much about the original data as it can by eavesdropping on the channel (*i.e.*, gradients). Such a setting is originally studied by Wyner in 1975 [33], and since then, quantifying the maximum capability of such attackers has been an active line of research.

However, a major requirement for fully understanding the attacker's capabilities is having complete knowledge about the data distribution, which is impractical for almost all multi-dimensional private datasets such as images or text. The other requirement is having power in designing and controlling a desirable channel, which is limited by other factors; e.g., one usually trains an off-the-shelf model that is already shown useful for similar tasks in collaborative learning. Overall, machine learning models, particularly DNNs used in practice, are

1) Forward propagation:

$$\{X,Y\} \longrightarrow T_1 \longrightarrow T_2 \longrightarrow \cdots \longrightarrow T_L$$

2 Backward propagation:

$$\ell(Y, T_L) \longrightarrow G_L \longrightarrow G_{L-1} \longrightarrow \cdots \longrightarrow G_1$$

$$\uparrow \qquad \qquad \uparrow \qquad \qquad \uparrow$$

$$T_{L-1} \longleftarrow T_{L-2} \longleftarrow \cdots \longleftarrow X$$

Fig. 2. Markov chain in forward propagation (from layer 1^{st} to L^{th}) and backward propagation (from layer L^{th} to 1^{st}). G refers to gradients; T refers to intermediate representations.

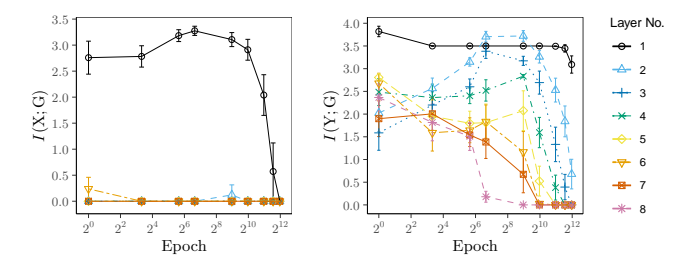


Fig. 3. Mutual information between each layer's gradients G and (left) inputs X, and (right) ground-truth label Y.

much larger and complicated than what can be fully understood for designing a secure communication.

Therefore, the typical procedure for quantifying information leakage is devising a specific attack and measuring its *success*. Such an attack-specific methodology lacks desirable theoretical justification and it is still unclear (i) how the attack success rate generalizes across different attackers, and (ii) what the exact dependence is on the attackers' knowledge and computational power. In this section, we explain our proposed methodology for generalizing attack success rate into an information-theoretic framework that improves our understanding of the attackers' capabilities as well as allowing us to categorize and compare different families of attacks.

4.1 Information Flow

There have been some efforts in understanding the flow of information in the forward propagation of a DNN, e.g., by analyzing intermediate representations of the input data in a layer-wise manner [34–36]. The visualization of data representations (i.e., layers' outputs) and model's parameters indicate that early layers mostly learn general information about data distribution (e.g., face color), while latter layers learn sample-specific information related to the underlying task (e.g., face identity) [18–20]. For theoretical justifications of such forward propagation analyzes, the widely

adopted method has been Shannon mutual information (MI or $I(\cdot;\cdot)$, hereinafter) [37, 38]. For an observed data sample X, labelled with Y, the layer-by-layer computations (from layer 1 to L) form a Markov chain (see Figure 2-①). According to the data processing inequality (DPI) [16], I(X;T) and I(Y;T) should not increase during the forward propagation, which is extensively studied for DNNs in [15–17] where authors show how to quantify information flow in forward propagation.

However, it is challenging (and we are not aware of any properly designed method) to apply similar methods for analyzing backward propagation. The computation of gradients (G_l) in the backward propagation form a more complicated Markov chain (see Figure 2-(2)), as it consists of (i) the gradients of loss function $(\ell(Y, T_L))$ and all previous layers (G_L, \ldots, G_{l+1}) , and (ii) the intermediate representations extracted by the forward propagation (T_{l-1}) . To build an intuition, we compute $I(X; G_l)$ and $I(Y; G_l)$ using the well-known MI neural estimation [39], for $l \in \{1, ..., 8\}$ on an 8-layer DNN [14] trained on MNIST [40] dataset for digit classification (see Figure 3). The results show that the first layer's gradients always have the highest MI for both X and Y. Latter layers have lower I(Y; G) except for the first several epochs.

4.2 The Role of Computational Power

The MI result in Figure 3 points out that the gradients of early layers contain more information about the original data X, and this is consistent with our theoretical and empirical expectation. However, this result also shows that early layers contain more information about label Y. Such an observation is not consistent with what is observed from practical attacks [6, 23, 41] and does not account for the fact that the latter layers may have done more processing on the data making the extraction of latent information easier.

More specifically, MI relies on the implicit assumption that "the attacker is computationally unbounded". If this is indeed the case, then both original and latent information are equally well-extractable from the first layer, as having given X we can theoretically infer any Y. For a computationally unbounded attacker, the information in the consequent layers can only decrease, in accordance with the data processing inequality. But in practice, the computational power and also the knowledge of the attacker is limited. One can then reasonably expect that the latter layers in a model are able to extract features that are more useful for the target task

(i.e., the classification at hand), so that usable information for the task Y, that is captured in the gradients, should be increasing throughout the layers. Consequently, one may also assume that other attributes besides the main task are also easier to extract from the latter layers. This would seemingly be in violation of the DPI; however, as we discuss next it can be reconciled under the framework of \mathcal{V} -information [26] which allows for usable information to increase throughout the network due to these computational constraints.

4.3 V-information

 \mathcal{V} -information is introduced [26] as a generalization of Shannon mutual information [37]. Here we adapt Vinformation to the attack success rate and show its application in measuring which layer(s) in a DNN carry more original or latent information. Specifically, Vinformation relies on a predictive family V, the definition of which allows incorporating various computational and knowledge constraints. Thus, the information contained in gradients about private variables becomes dependent on the model used to extract such information. Without any constraints on the family of the attack models, \mathcal{V} -information is equivalent to MI; i.e., if we consider an attacker using a predictive family that includes all predictive models. The ability to include constraints, such as considering a specific family of attackers, allows measuring information that is only usable to that family while accounting for their computational power and forming the basis for better understanding what private information can be extracted for what type of attackers.

The setting considered is as follows: a computationally bounded adversary, denoted as A, is trying to predict the outcome of a real-valued random variable, e.q., private original data X or latent information p using any subset of the shared gradients G as side information. Let $f[g_{l,i}]$ be a probability distributions over the sample space of X (hereafter \mathcal{X}) chosen based on the received gradient information $g_{l,i}$ from layer l and neuron i. Similarly, let $f[\emptyset]$ denote the prior distribution given no gradient information \emptyset . Then, $f[g_{l,i}](x) \in \mathbb{R}$ is the value of the density evaluated at $x \in \mathcal{X}$, i.e., f evaluated at x is the probability of observing the true value x given a particular gradient sample $g_{l,i}$. The first definition we need is that of a predictive family, which defines the set of models that an attacker is able to use based on the attackers computational and knowledge constraints:

Definition 1 (Predictive family [26]). \mathcal{V} is a predictive family if for any model $f \in \mathcal{V}$ and any $Q \in \text{range}(f)$ there exists an $f' \in \mathcal{V}$ such that for any $x \in \mathcal{X}$, f'[x] = Q and $f'[\emptyset] = Q$.

This means that the model can ignore side information if needed.

Examples of predictive families. Below we present several examples of predictive families successfully used as attack models. We remark once more that finding the best-performing model in a predictive family satisfying Definition 1 allows to reason about the information loss for any model in that family.

- 1. **Linear regression.** Let $x \in \mathbb{R}^d$. Define $f(x) = \mathcal{N}(\sum_{i=1}^d a_i x_i + b, \sigma)$ and $f(\emptyset) = \mathcal{N}(c, \sigma)$. Then an f' which satisfies Definition 1 is given by setting $a_i = 0$ for i = 1, ..., d and b = c. This can be generalized to e.g. polynomial regression.
- 2. **Neural network.** Let f(x) be a L-layer network with bias b_i in layers i = 1, ..., L. Suppose we have P nodes in the final layer and the final output is processed through a softmax to obtain a distribution. Let $f(\emptyset)$ be a uniform distribution with probabilities 1/P for all output nodes. Then an f' which satisfies Definition 1 is given by a model with all weights equal to zero and all bias values equal to a constant as its output will be exactly that of $f(\emptyset)$ i.e., 1/P.

We then have the following definition of empirical V-information.

Definition 2 (Empirical V-information [26]). For original information X the empirical V-information over gradients $g_{l,i}$ is computed using,

$$\hat{I}_{\mathcal{V}}(G \to X; \mathcal{D}) = \inf_{f \in \mathcal{V}} \frac{1}{|\mathcal{D}|} \sum_{\mathbf{x}_i \in \mathcal{D}} -\log f[\emptyset](\mathbf{x}_i)$$
$$-\inf_{f \in \mathcal{V}} \frac{1}{|\mathcal{D}|} \sum_{\mathbf{g}_{l,i}, \mathbf{x}_i \in \mathcal{D}} -\log f[\mathbf{g}_{l,i}](\mathbf{x}_i).$$
(6)

For latent information (attribute) P the same equation holds with X and x_i replaced by P and p_i . V-information thus requires computing the difference between the probability of recovering private information X or P using the best attack model in a specified predictive family V. It is shown that for the family of empirical risk minimizers, the best model (imposed by inf in (6)) can be found using e.g., SGD [26]. Intuitively V-information quantifies the (private) information obtained by the attacker through observing gradients.

For a predictive family including only one attack model, computing \mathcal{V} -information is similar to computing the attack success rate for that attack model. But \mathcal{V} -information give us a framework to provide the guarantee that the upper bound on information leakage holds for the full attack family, by quantifying the success rate of the best model in that family. In the next sections we show how to define probability distributions over both the latent information and original information.

Probability distribution for latent information.

We will use v to denote the attackers' model taking as input the gradient so that $v(\mathbf{g}_{l,i})$ is its output. To apply \mathcal{V} -information to latent information leakage one requires the definition of a probability distribution over the inferred attributes. Here we briefly discuss how to obtain such a probability distribution. For latent information the label \mathbf{y}_i for sample i is given by the presence or absence of an attribute, i.e. $\mathbf{p}_i \in \{0,1\}$. We remark that this can easily be generalized to more than two attributes. Training a model with a softmax output layer gives a probability distribution over the layers output values. In other words, to obtain the probability distribution over latent information we will use,

$$f_{\mathcal{A}}[\mathbf{g}_{l,i}](\mathbf{p}_i) = \frac{e^{\{v(\mathbf{g}_{l,i})\}_{\mathbf{p}_i}}}{e^{\{v(\mathbf{g}_{l,i})\}_0} + e^{\{v(\mathbf{g}_{l,i})\}_1}},\tag{7}$$

and $f_{\mathcal{A}}[\emptyset](\mathbf{p}_i) = \frac{1}{2}$, *i.e.*, the value of the uniform distribution over the outputs.

Probability distribution for original information.

Similar to latent information, to apply \mathcal{V} -information for original information leakage, a probability distribution over the true labels, in this case the true original information, needs to be defined. Here, the label y_i is a particular input sample x_i , *i.e.*, the original input used in the model. We construct the probability distribution using a Gaussian distribution; this is motivated by the various relationships between Gaussian posteriors and the minimization of the mean squared error (see *e.g.*, Section 3.3.1 in [42]). Due to the high dimensionality of the image we choose to replace the distance from the mean in the exponential with the structural similarity index measure (SSIM) [43]. We obtain the following approximation of a density.

$$f_{\mathcal{A}}[\mathbf{g}_{l,i}](\mathbf{x}_i) = \frac{1}{\sqrt{2\pi\sigma}} e^{-\frac{(1-\text{SSIM}(v(\mathbf{g}_{l,i}),\mathbf{x}_i))^2}{2\sigma^2}},$$
 (8)

where $SSIM(v(g_{l,i}), x_i)$ measures the perceptional similarity between reconstructed and original data, such that 1 - SSIM gives the dissimilarity. Regarding other types of data one can adopt measures in similar ways (e.g., Peak Signal-to-Noise Ratio for audio). SSIM can

be computed as a combination of luminance (l), contrast (c), and structure (s):

$$SSIM(v(\mathbf{g}_{l,i}), \mathbf{x}_i) = l(v, \mathbf{x}_i)c(v, \mathbf{x}_i)s(v, \mathbf{x}_i), \tag{9}$$

where we suppress the dependence of v on $g_{l,i}$. Functions of l(.), c(.), and s(.) are determined by the average and variance of both $v(g_{l,i})$ and x_i and their covariance (see [43] for details). This similarity is 0 for the worst prediction, and thus, $f_{\mathcal{A}}[\emptyset](x_i) = e^{-2\pi^2}$ for $\sigma = \frac{1}{2\pi}$.

5 Towards attack-independent quantification

While the attack success rate and its theoretical generalization \mathcal{V} -information are able to quantify the privacy leakages in gradients for both latent and original information, it depends on the specific (family of) attack models chosen. To better understand information leakages and design effective protection mechanisms, it is desirable to make no explicit assumptions about the attackers' model while still obtaining insight into which characteristics of neural networks make it more sensitive to privacy leaks and how these privacy leaks happen.

5.1 Sensitivity

We begin with a metric based on sensitivity to quantify original information leakage from the gradients i.e., sensitivity of the gradient w.r.t. the input. Consider again the objective in (1). It is clear that if the objective function has many local minima, solving the optimization and thus recovering the data exactly will not be possible. Therefore, the success of the recovery depends on the structure of the objective function. Previous work has introduced rank-based metrics to quantify the ability to find the unique optimizer [3] relying on the fact that the optimization problem can be rewritten as a system of equations. If more parameters exist than equations, no unique solution will exist. Alternatively, one could choose a metric that accounts for the flatness of the loss function (and hence the gradients) in parameter or input space. This generalizes the notion of multiple local minima to also allow for flat minima, a common occurrence in the loss functions of deep neural networks[44]. This notion of sensitivity based on flatness has been applied in measuring model robustness on adversarial example attacks [45, 46]. A model that is non-sensitive to certain changes in inputs is expected to have high robustness.

On the other hand, by bounding the sensitivity of outputs w.r.t. inputs leveraging differential privacy, one can certify model robustness to changes in input i.e., adversarial examples, proposed in [47].

Thus we use the following intuition to measure leakage: if the gradient sensitivity is low and thus gradients change insignificantly when altering the input, reconstructing the input will be more challenging. More specifically, we can utilize the Jacobian matrix of the gradients w.r.t. the input (similar to input-output Jacobian [48, 49]) to reflect how sensitive the gradients are when changing the input, *i.e.*, a sensitivity measure on gradients. The input-gradient Jacobian is calculated by:

$$\mathbf{J}_{l}^{(G)}(\boldsymbol{X}) = \frac{\partial \mathbf{g}_{l}(\boldsymbol{X})}{\partial \boldsymbol{X}} = \frac{\partial}{\partial \boldsymbol{X}} \left(\frac{\partial \ell(\boldsymbol{X}, \boldsymbol{y}, \boldsymbol{\theta})}{\partial \boldsymbol{\theta}_{l}} \right), \quad (10)$$

where $\mathbf{g}_l(.)$ represents the function that produces layer l^{th} 's gradients G_l . Besides, $\ell(.)$ is the loss function over X, ground truth y, and parameters of the complete model θ , so $\mathbf{g}_l(.)$ can be regarded as the partial derivative of $\ell(.)$ w.r.t. layer l^{th} 's parameters θ_l (i.e., backward propagation).

Then we compute the Frobenius norm (referred to F-norm) of the above input-gradient Jacobian matrix similar to [48], which indicates the general input leakage risk. As in our case Jacobians are compared across layers with different sizes, we include two other norms, i.e., 1-norm and the ∞ -norm. Using different norms will help in capturing adversaries with different capabilities, similar to the differential privacy in adversarial example [47, 50], where the p-norm reflects how the adversary measures distance between two data samples (e.g., 1norm considers all dimensions of the data sample, and ∞ -norm focuses on one dimension). Thus, given K data samples, we compute the Jacobian with p-norm (referred to as 'Jacobian p-norm' hereinafter) averaged over the data samples as the leakage risk of the original information (X) in layer l^{th} 's gradients:

$$\mathcal{R}_{l}^{(\boldsymbol{X})} = \mathbb{E}_{\Delta \boldsymbol{X}} \left[\| \mathbf{g}_{l}(\boldsymbol{X}) - \mathbf{g}_{l}(\boldsymbol{X} + \Delta \boldsymbol{X}) \|_{p} \right]$$

$$= \frac{1}{K} \sum_{l=1}^{K} \left\| \mathbf{J}_{l}^{(G)}(\boldsymbol{X}_{k}) \right\|_{p}$$
(11)

where $p = F, 1, \text{or } \infty$. Note that the size of G_l still has an impact on the computed sensitivity. A larger G_l size can result in a larger sensitivity in terms of 1-norm and F-norm. When reconstructing high-dimensional input data, a large G_l size is necessary, which can be reflected by these norms.

5.2 Subspace distances

For attacks on latent information, such as the attribute inference in [5], the success of the attack lies in the ability of the classifier to distinguish between whether certain gradients were computed over data that did or did not have a certain attribute. Specifically, as discussed in Section 3.2 it relies on how accurate the classifier trained on samples with or without an attribute can become. One may consider again computing the sensitivity of gradients w.r.t. latent information (the attributes). However, this is intractable because i) this latent information is not in the machine learning computational graph so to compute $\frac{\partial \mathbf{g}}{\partial \mathbf{p}}$ is not straightforward, and ii) a large number of inputs have the same latent information, and based on that, the attack's classifier only produces a binary prediction, while sensitivity (e.g., in Equation (11)) measures each data point separately. Sensitivity is thus a too local measure to grasp the amount of latent (i.e., coarse) data in the gradients. Therefore, to quantify the changes in gradients, we follow a more coarse-grained approach. First, we separate the target dataset into two parts based on the presence of one specific latent information, and then we compare the subspace distance between gradients computed on these two parts of the dataset. This still follows the same intuition as understanding how sensitive the gradients are w.r.t. latent information but considers a more 'high-level' measurement.

Without loss of generality, assume that dataset S consists of two disjoint subsets S_0 , whose samples do not have the target latent information, and S_1 , whose samples have the target latent information. Then we obtain the corresponding gradients of layer l^{th} computed on these two subsets by:

$$G_l^{(0)} = \mathbb{E}_{X \in \mathcal{S}_0}[\mathbf{g}_l(X)] \text{ and } G_l^{(1)} = \mathbb{E}_{X \in \mathcal{S}_1}[\mathbf{g}_l(X)].$$
 (12)

For each pair of matrices $G_l^{(0)}$ and $G_l^{(1)}$ (in $l \in \{1,...,L\}$), let $\mathbb{G}_l^{(0)}$ and $\mathbb{G}_l^{(1)}$ denote their corresponding subspaces, respectively. To measure the difference between the computed gradients with and without target latent information, we can compute the Grassmann geodesic distance [51, 52] between these two subspaces as the leakage risk of this latent information p in layer l^{th} 's gradients:

$$\begin{split} \mathcal{R}_{l}^{(p)} &= \mathrm{dist}(\boldsymbol{G}_{l}^{(0)}, \boldsymbol{G}_{l}^{(1)}) = d_{\mathrm{Gr}(k,n)}(\mathbb{G}_{l}^{(0)}, \mathbb{G}_{l}^{(1)}) \\ &= \left(\sum_{i=1}^{k} \theta_{i}^{2}\right)^{1/2}, \end{split} \tag{13}$$

where $\operatorname{Gr}(k,n)$ denotes the Grassmann manifold, and both $\mathbb{G}_l^{(0)}$ and $\mathbb{G}_l^{(1)}$ are elements of $\operatorname{Gr}(k,n)$ and are k-

dimensional linear subspace in \mathbb{R}^n . k is the layer l^{th} 's gradient size $N_l \times N_{l-1}$. θ_i for $i \in \{1, ..., k\}$ are principal angles between the two subspaces which can be computed using numerical methods [53]. In this paper we use the Grassmann distance; other common distances defined on Grassmannians (e.g., Asimov) [52] can be derived similarly.

6 Numerical results

In this section, we analyze the information leakage from gradients using the proposed quantities (\mathcal{V} -information, sensitivities and gradient subspaces) to better understand in what situations leakage happens. Our analysis is performed on multiple models and datasets and using different training schemes.

6.1 Evaluation Setup

Model. We consider several different models on whose gradients the leakage will be studied. First, the LeNet has two convolutional (Conv) layers with 6 and 16 filter, respectively, of 5×5 size (and each has a max-pooling with a size of (2,2) after). Then it is followed by three FC layers with 120, 84, and d_y neurons. d_y is the output size or the number of classes. Second, the AlexNet has five Conv layers with 8, 16, 32, 32, and 32 filters. The first is with size 5×5 and the others are with size 3×3 . The second and the fifth have a max-pooling with a size of (2,2) after, followed by three FC layers same as the LeNet. Third, the VGG9 has five Conv layers with 8, 16, 16, 32, 32, and 32 filters of 3×3 size. The third and the sixth have a max-pooling with a size of (2,2) after. Then it is followed by three FC layers with size of 256, 128, and d_y , respectively. All three models use ReLU activation functions for all layers (except the output layer with Softmax). Lastly, the considered TextClf has two Conv layers followed by two FC layers. Conv layers have 16 filters with size 3 and 8 respectively, and each has a maxpooling with a size of 2 after. FC layers have 50 and d_y neurons respectively.

Datasets. LeNet, AlexNet, and VGG9 models are trained on CIFAR-100 [54] and three other image datasets with attributes, including Labeled Faces in the Wild (LFW) [55], Large-scale CelebFaces Attributes (CelebA) [56], and Public Figures Face Database (Pub-Fig) [57]. The last model (i.e., TextClf) is trained on two text datasets: IMDB reviews [58] and CSI corpus [59].

LFW contains 13233 face images (cropped as 62×47 RGB). All images are labeled with around 100 attributes such as gender, race, age, hair color, etc. CelebA contains more than 200k face images of celebrities with 40 attribute annotations such as gender, hair color, eyeglasses, etc. We use a subset of the cropped version (i.e., 15000 images) and resize images to 64×64 RGB. We also use a cropped version (100×100 RGB) of PubFig which contains 8300 facial images made up of 100 images for each of 83 persons [60]. All images are marked with 73 attributes (e.g., gender, race, etc). In IMDB reviews [58] dataset, each review is labeled with sentiment and length, and in CSI corpus [59], each corpus review is labeled with sentiment, veracity, length, grade, etc.

Attributes for measuring latent information. For all datasets, we select a subset of attributes considered as private in our evaluation. In Table 2, for each item of name 'a_b_c', 'a' refers to the dataset, 'b' refers to the classification task, and 'c' refers to the attribute considered as private latent information.

Training setup. We conduct our experiments on a cluster with multiple nodes where each has 4 Intel(R) Xeon(R) E5-2620 CPUs (2.00GHz), one/two NVIDIA RTX 6000 GPU(s) (24GB), and 24GB/48GB DDR4 RAM. Pytorch v1.4.0 is used for DRAs, sensitivity and subspace distance computations, and Theano v1.0 is used to conduct AIAs. Regarding \mathcal{V} -information on the data reconstruction and the attribute inference, attacks can start from the beginning of training process by default. We refer to our codes for more details of gradient change measures and [4, 5] for attack settings.

6.2 Layer-wise information leakages with Vinformation

Here we deploy V-information to measure the maximum original and latent leakage for selected attack families.

Attack families. In order to use the \mathcal{V} -information we need to define an attack family and consequently compute the empirical \mathcal{V} -information as in Equation (6). For the latent information we will select a random forest as the attack family with the hyperparameters tuned in a state-of-the-art manner based on previous successful attacks [5]. For original information we will use a deep neural network trained with SGD as in previous attacks [3, 4]. The probability distributions are used as explained in Section 4.3.

Original information by V-information. To measure layer-wise information leakage, we perform attacks

Table 2. Settings of dataset, tasks, and attributes in latent information-related experiments.



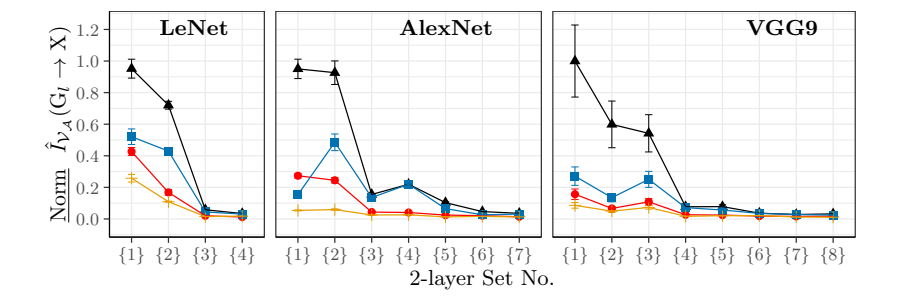


Fig. 4. Original information leakage risks, measured by \mathcal{V} -information, in each 2-layer set's gradients, based on CIFAR100 (—), LFW (—), CelebA (—), PubFig (—) datasets. Error bars are 95% confidence intervals. 20 trails hereafter.

on individual layers. As we found that existing DRAs are not successful when using gradients of only one layer, we measure this leakage on the set of two consecutive layers at a time. Specifically, in Figure 4, set {1} denotes layers 1st and 2nd, set {2} denotes layers 2nd and 3rd, etc. Furthermore, we normalize the computed V-information of one model with the maximum value of its layer for comparability across models and tasks. The results indicate that the original information leakage risk generally decreases when moving from the first 2-layer set to the last 2-layer set, although there exist slight fluctuations. This decreasing pattern agrees with the Markov chains in the Figure 3, where for both forward and backward propagation, G₁ and G₂ are closest to the X and T₁; thus encoding the most information original data. Besides, the information leakage risk for CIFAR100 is higher than for the other three face-image datasets. This could be due to the fact that in CIFAR100 images of different objects have richer features (e.g., ambient colors and shapes) than face images, leading to more significant gradient changes that are easier to capture by attack models.

Latent information by V-information. For latent information, we additionally train the TextClf on the two text datasets and remove CIFAR100 because it does not have multiple attributes. Also, since each dataset can have multiple types of attributes considered as private latent information, we compute V-information on all these attributes and then fit smooth curves us-

ing nonparametric local weighted (i.e., LOESS) regression [61] to clarify the general trend across layers. As shown in Figure 5, the latent information leakage risk follows a trend that increases when moving through the feature extractor layers, reaches its maximum at the first classifier layer, and then decreases. This result is similar across all models. Compared to MI in Figure 3, the results from V-information are more reasonable and in accordance with the attack results. The reason is that measuring with V-information considers computational constraints of the attacker. More interestingly, the exact original information (i.e., what is the exact input) mostly lies in the first layers as our analysis shows, and most existence/membership information (i.e., whether this input exists in the training set or not) and classification task information (i.e., labels) are in the last layers as found in previous research [6, 23, 41, 62], so it is expected that the latent information (i.e., which attribute the input has) would be extracted from the middle layers.

6.3 Attack-independent information leakages

Here we localize information leakages by measuring the gradient changes. This measure is used directly on the trained model and is thus attack-independent.

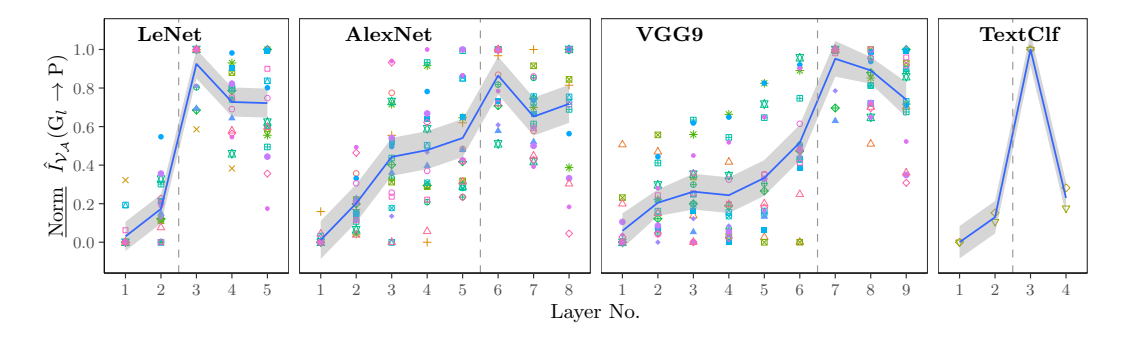


Fig. 5. Latent information leakage risks, measured by \mathcal{V} -information, in each layer's gradients. Scattered points refer to private attributes being measured for different datasets and classification tasks. Blue lines give the LOESS regression curve. Dashed lines (--) separate the feature extractor and the classifier of the model.

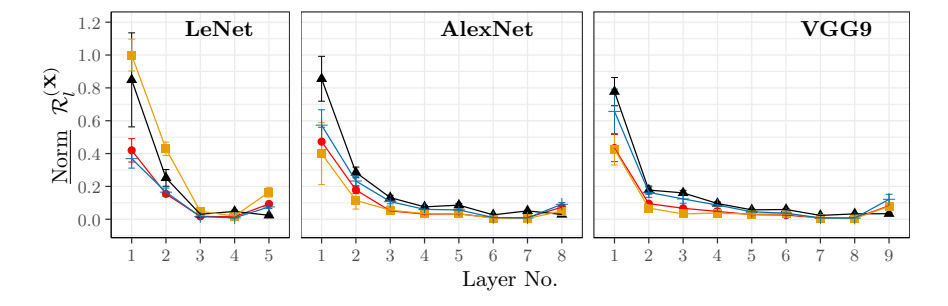


Fig. 6. Original information leakage risks, measured by sensitivity, in each layer's gradients, based on CIFAR100 (—), LFW (—), CelebA (—), PubFig (—) dataset. Error bars are 95% confidence intervals.

Original information. We compute Equation (11) to measure original information leakage risks. As shown in Figure 6 for the F-norm, overall the sensitivity shows a similar pattern as V-information (in Figure 4). Specifically, gradients of the first layers are more sensitive to changes in inputs compared to latter layers, thus they could potentially carry more private original information that can be detected by adversaries easier. Besides, the result of sensitivity shows that models trained on several datasets (e.g., CIFAR100) can have higher leakage risks than others, which is close to the results of V-information in general. There are small differences between results of \mathcal{V} -information and sensitivity measure, both in the order of specific datasets (e.g., LeNet on PubFig) and in the specific value of layers' information leakage risks, which may be due to that attack models cannot capture all changes in the gradients or there are influence factors other than sensitivity.

When computing sensitivity, we can use measures with different p-norm to reflect the ability of attackers. In Figure 8, we show 1-norm and ∞ -norm sensitivity. The results generally show similar patterns with the results of F-norm sensitivity in Figure 6: First layers have higher original information privacy risks.

Latent information. We compute Equation (13) to measure latent information leakage risks. Similar to V-

information, we measure all possible attributes of used datasets and again plot the regression curves for each model. As Figure 7 shows, $\mathcal{R}_{l}^{(p)}$ generally follows a similar trend as the latent information risks computed using \mathcal{V} -information. That is, the layers related to the classifier have higher leakage risks than the feature extractor layers. Most risks are either in the classifier's first layer or the second layer. While this is slightly different from the results in Figure 5 where the first layer always has the highest leakage, the overall trend remains the same. We also notice that several scattered points closely coincide, and the last layer has a lower risk compared to that in V-information. One explanation is that this measure may tend to capture the extreme risks among layers so the first and second layers of the classifier show significantly higher leakage risks than the other layers. Overall, the computation measuring gradient changes (i.e., both sensitivity and subspace distance) depends only on the gradients, is easy-to-compute and captures the main pattern of layer-wise leakage risks measured by attack-based V-information.

Validation of gradient change metrics. We validate the success of gradient change metrics based on the theoretically-grounded \mathcal{V} -information. The gradient change metrics are computed directly on the trained model, and thus do not depend on the chosen attack

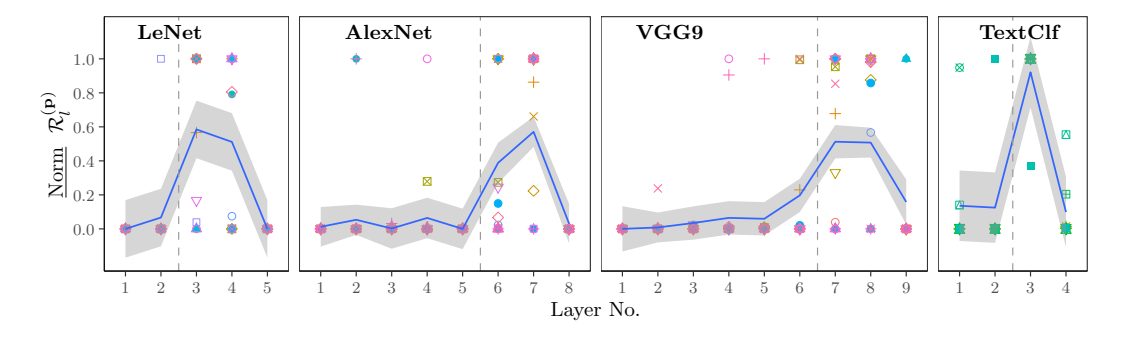


Fig. 7. Latent information leakage risks, measured by subspace distances, in each layer's gradients. Scattered points correspond to private attributes. Blue lines give the LOESS regression. Dashed lines (--) refer to the feature extractor-classifier connection.

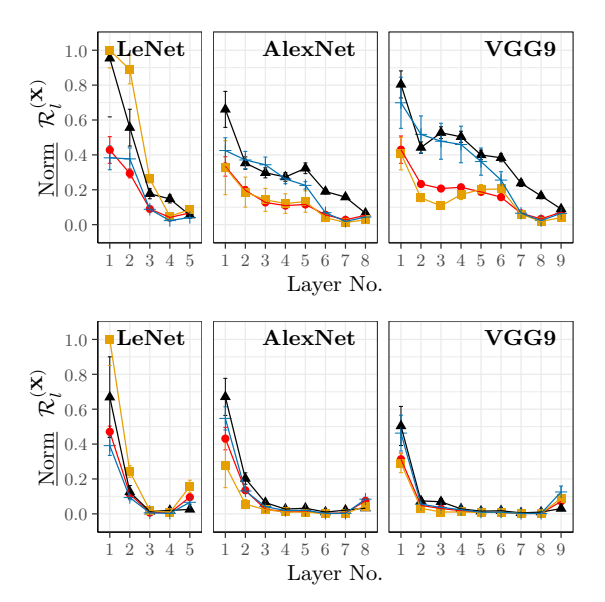


Fig. 8. Original information privacy risks, measured by sensitivity ([Top] 1-norm; [Bottom] ∞ -norm), in each layer's gradients, based on CIFAR100 (—), LFW (—), CelebA (—), PubFig (—) dataset. Error bars are 95% confidence interval.

family. Our correlation analysis shows that the results between gradient change metrics and \mathcal{V} -information are with medium to high correlation: $R=0.686\sim0.707$ with p<0.003. The fact that their values coincide with \mathcal{V} -info shows that one can reason about information leakages that include different attack models, and by computing metrics directly on the model gradients one has the benefit being that it does not require the definition and computation of an attack.

6.4 Hyperparameter impacts

Next, we further explore how the most common training hyperparameters, *i.e.*, aggregation levels and training epochs, affect gradient-based information leakages.

Aggregation levels. Performing aggregation before sharing gradients with others is a very common strategy in federated learning. This could be the local aggregation (e.g., batch size in FedSGD or multiple steps in FedAvg) and also the global aggregation over updates of all clients. For our aggregation measurement on one target's (victim) original or latent information, we mix it with multiple gradients of non-target information, i.e., information irrelevant to the private information targeted by adversaries. Our empirical results show that aggregation can significantly reduce gradients' information leakage risks (see Figure 9). Specifically, disclosing target original information from gradients that have been updated on non-target information that is 10 times the amount of target information can be very difficult (e.g., a batch size of 10 in [3, 4]). When gradients are mixed with non-target information that is 30 times the amount of target information, the original information risk measured by sensitivity is extremely low (near zero). Also, extracting latent information from $30\sim50$ times non-target information is hard (e.g., $30\sim50$ participants in [5]).

Epochs. We measure the information leakage risks of gradients at specific epochs (from 1 to 100) during training. Overall the epoch only has a negligible impact on leakage risks (see Figure 10). Except for the leakage risk drop in the first several epochs (i.e., first 10 epochs for original information and first 20 epochs for latent information), epochs barely change gradients leakage risks. This may be due to the fact that the magnitude of the updated gradients does not change significantly throughout these epochs (for fixed learning rate). In such a sense, in the first epochs, the machine learning optimizer quickly converges somewhere near the optimum and increases the model accuracy very quickly; in later epochs, the optimization becomes slower, and consequently, the magnitude of gradient changes stabilizes.

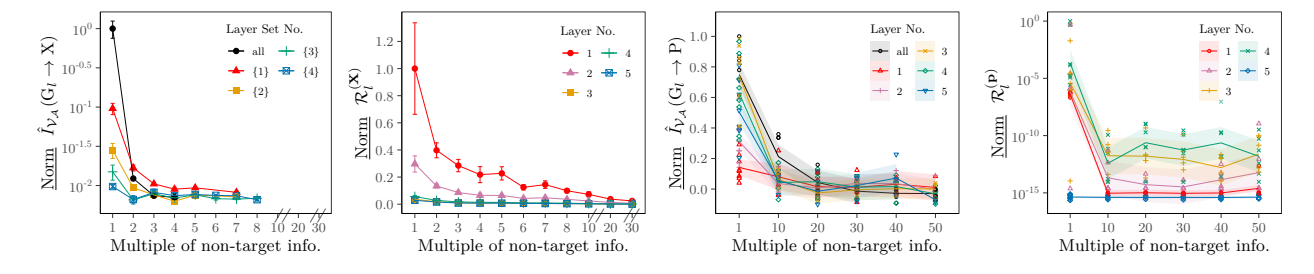


Fig. 9. Influence of gradient aggregation on risks of original information [Left two] and latent information [Right two], measured on LeNet trained on CIFAR100 and LFW, respectively (Note: Points corresponding to failed trials of attacks are not plotted. Logarithmic scale is used in some plots for better visualization).

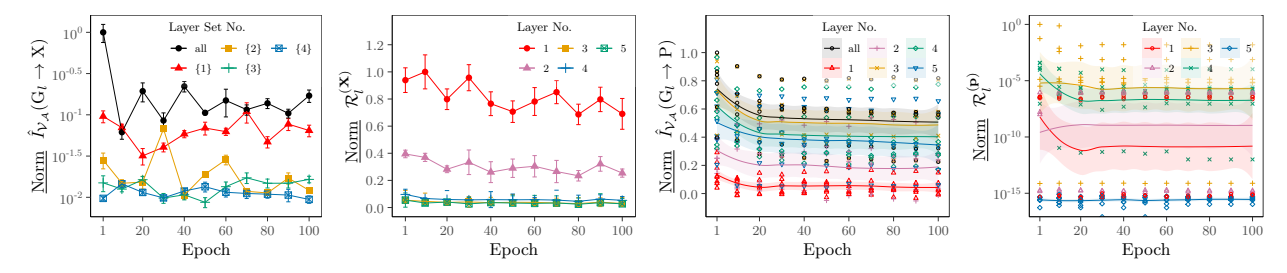


Fig. 10. Influence of training epoch on risks of original information [Left two] and latent information [Right two], measured on LeNet trained on CIFAR100 and LFW, respectively.

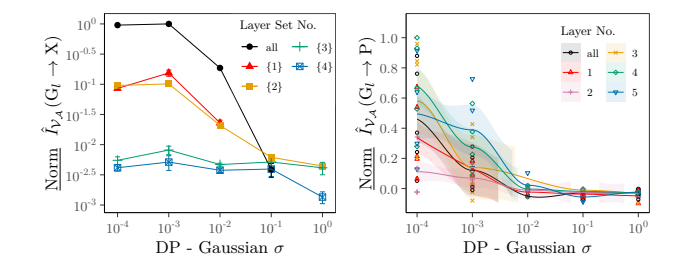


Fig. 11. Influence of training epoch on risks of original information [Left] and latent information [Right], measured on LeNet trained on CIFAR100 and LFW, respectively.

This also confirms that gradient changes can be a highly important factor related to private information leakages. Differential privacy. Adding differentially private (DP) noises before releasing gradients could be one way to reduce the privacy risks. Here we follow [21, 63], i) to clip gradients using l2-norm and then ii) to add Gaussian noises. Specifically, we set the max norm as 1 for all cases and adjust the standard deviation σ of Gaussian noises from 10^0 to 10^{-4} . Noises are only added every time before releasing gradients; that is, pre-sample noise addition for data reconstruction attacks, pre-batch (32) samples) noise addition for attribute inference attacks. We do not tune training hyperparameters or report the privacy budget of this DP training for simplicity. Note that adding noises to gradients does not change the derivative results of $\frac{\partial \mathbf{g}_l(\mathbf{X})}{\partial \mathbf{X}}$, i.e., sensitivity, we give the \mathcal{V} -information measure below. The empirical results are

given in Figure 11 and show that DP can reduce the privacy risks of both original and latent information, due to the fact that noises can perturb information in gradients. In addition, adding noises to the first layers tends to have higher effectiveness in alleviating original information risks, as the risks do not change significantly in terms of the last layers. Similarly, noises could provide better protection in the last layers when it comes to latent information. This again highlights the locations of different types of information and the needs of potential layer-wise DP protection.

7 Discussion

On the localization of the most sensitive nodes.

The location of the most sensitive nodes in a model can change depending on the type of information. More specifically, our analysis showed that the nodes in the first layer contain the most sensitive information of the original input which is supported by previous findings [3, 8]. Regarding latent information, we found that the first FC layers (typically placed after the last Convlayer) are the most sensitive layers. One explanation for this is that latent information between the original information, X, and output information, Y, is best captured in a middle layer. In addition, an attribute is a high-level feature; the FC layer classifies the feature maps from the

previous Conv layers, and it can contain distinguishable high-level latent information such as the property. Similarly, the last Conv layer is likely to have more latent information than previous Conv layers, because initial Conv layers learn more general information (e.g., ambient colors or edge in images), while latter Conv layers focus on high-level latent information (e.g., face identity) [18, 19].

On the insights gained from gradient-based measures. We showed that adopting V-information results in a useful theoretical framework that generalizes attack success rates by guaranteeing that the maximum information loss will be only as big as the information loss for the best attacker in a family of attack models. We then introduced sensitivity and subspace distances as measures that are independent of a chosen attack family with the goal of further understanding how and what kind of information leakages happen. Sensitivity is a local measure that allows accounting for flatness in the objective function minimized in DRA attacks (Equation (1)). This flatness is known to occur in neural network loss functions [44], and therefore the proposed sensitivity metric can be a valuable tool in understanding sensitive information leakage. In addition, a low sensitivity has been linked to increased robustness of trained models [49]. Adapting the tools that were consequently introduced to improve robustness can help design better defenses against original information leakage. The gradient subspace distances are a novel metric introduced with the aim of capturing more coarse-grained information. As sensitivity in itself is a local measure to capture latent information leakages, subspace distances are a valuable extension. Defined as the distance between gradients with and without target information, it helps inform in which trained models leaks can happen, or in other words whether the weights of the models are trained in such a way that they are able to distinguish between attributes.

On using localization for the design of protection mechanisms Our characterization allows us to localize which nodes in which layers leak most sensitive information. This highlights opportunities for designing defenses that are flexible and practical at a nodewise level. For example, fully homomorphic encryption (FHE)-based approaches fully respect the model privacy but it leads to high runtime overhead. Our analysis can be used towards solutions utilizing FHE only on the sensitive part of the model during training. In addition, given the resource constraints on edge devices, TEE-based approaches with model partitioning have also be-

come a promising approach. Specifically, during learning, one can deploy and run the most sensitive layers (e.g., the last Conv layer and the first FC layer) inside the TEE using model partitioned execution techniques across trusted and untrusted environments similar to [23]. Our measures could also provide insights for layer-wise, federated training of models [24, 64], which could further reduce the privacy risk by exposing only specific layers instead of the complete model.

Furthermore, there are privacy-preserving techniques proposing to add noise to gradients (*i.e.*, DP), share fewer gradients, or use dimensionality reduction and regularization (*e.g.*, Dropout). However, none of them can protect against latent or original information leakage without significantly compromising model utility [3, 5]. The ability to localize the most sensitive nodes can allow adding noise only where necessary. As one example, clipping or adding noises differently for layers in DP [22, 65] and directly hiding layers in TEEs [23, 25] could be one promising protection without compromising the utility of the other layers and our quantification helps in understanding and designing these layer-wise protection mechanisms.

8 Conclusions

Quantifying the information flow in backward propagation and information leakages associated with the computed gradients is still a conundrum, as it remains unclear in what part of the model, and for what kind of attacks, leakages happen. Attack success rates are the standard way of measuring an attacker's ability to extract sensitive information from shared gradients, however, this clearly depends on a particular attack. This handicaps our ability to reason about the amount of leakage in an attack-independent manner. In this paper, we presented a framework that encompasses the attack success rate but generalizes it by measuring the information loss from gradients over a certain family of attack models. Taking step into the direction of attackindependent understanding of leakages, we also presented gradient-based metrics. These metrics work directly on the trained model and are motivated by the mathematical formulation of successful attacks. Empirical results show that our layer-wise analysis provides a better understanding of the memorization of information in neural networks and facilitates the design of flexible layer-level defenses for establishing better tradeoffs between privacy and costs. Specifically, we introduced mathematically-grounded tools to better quantify information leakages, and applied these tools to localize sensitive information in several models over different datasets and using different training hyperparameters.

Future works. i) It is expected that DNNs with skip connections (e.g., ResNet [66]) could give similar results because they usually have a unidirectional gradient flow, but this needs further experiments. Information leakages in other widely used networks such as Recurrent [67] or Graph [68] neural networks need investigating; ii) More defense mechanisms can be analyzed using our proposed metrics. For example, the influence of differential privacy can provide a further understanding of the linkage between information leakages and gradient changes; iii) Factors other than sensitivity deserve further exploration. Bayesian-based generalization analysis [69] may help to theoretically characterize information leakages from another perspective.

References

- B. McMahan, E. Moore, D. Ramage, S. Hampson, and B. A. y Arcas, "Communication-efficient learning of deep networks from decentralized data," in *Artificial Intelligence and Statis*tics, 2017, pp. 1273–1282.
- [2] Q. Yang, Y. Liu, T. Chen, and Y. Tong, "Federated machine learning: Concept and applications," ACM Transactions on Intelligent Systems and Technology (TIST), vol. 10, no. 2, pp. 1–19, 2019.
- [3] L. Zhu, Z. Liu, and S. Han, "Deep leakage from gradients," in Advances in Neural Information Processing Systems, 2019, pp. 14747–14756.
- [4] B. Zhao, K. R. Mopuri, and H. Bilen, "iDLG: improved deep leakage from gradients," arXiv preprint arXiv:2001.02610, 2020.
- [5] L. Melis, C. Song, E. De Cristofaro, and V. Shmatikov, "Exploiting unintended feature leakage in collaborative learning," in 2019 IEEE Symposium on Security and Privacy (SP). IEEE, 2019, pp. 691–706.
- [6] M. Nasr, R. Shokri, and A. Houmansadr, "Comprehensive privacy analysis of deep learning: Passive and active white-box inference attacks against centralized and federated learning," in 2019 IEEE Symposium on Security and Privacy (SP). IEEE, 2019, pp. 739–753.
- [7] A. Salem, A. Bhattacharya, M. Backes, M. Fritz, and Y. Zhang, "Updates-leak: Data set inference and reconstruction attacks in online learning," in 29th {USENIX} Security Symposium, 2020, pp. 1291–1308.
- [8] J. Geiping, H. Bauermeister, H. Dröge, and M. Moeller, "Inverting gradients—how easy is it to break privacy in federated learning?" arXiv preprint arXiv:2003.14053, 2020.
- [9] H. Yin, A. Mallya, A. Vahdat, J. M. Alvarez, J. Kautz, and P. Molchanov, "See through gradients: Image batch recovery via gradInversion," arXiv preprint arXiv:2104.07586, 2021.
- [10] H. Ren, J. Deng, and X. Xie, "GRNN: Generative regression neural network—a data leakage attack for federated learning," arXiv preprint arXiv:2105.00529, 2021.
- [11] S. Yeom, I. Giacomelli, M. Fredrikson, and S. Jha, "Privacy risk in machine learning: Analyzing the connection to overfitting," in 2018 IEEE 31st Computer Security Foundations Symposium (CSF). IEEE, 2018, pp. 268–282.
- [12] K. Leino and M. Fredrikson, "Stolen memories: Leveraging model memorization for calibrated white-box membership inference," in 29th {USENIX} Security Symposium, 2020, pp. 1605–1622.
- [13] N. Carlini, C. Liu, Ú. Erlingsson, J. Kos, and D. Song, "The secret sharer: Evaluating and testing unintended memorization in neural networks," in 28th {USENIX} Security Symposium, 2019, pp. 267–284.
- [14] A. M. Saxe, Y. Bansal, J. Dapello, M. Advani, A. Kolchinsky, B. D. Tracey, and D. D. Cox, "On the information bottleneck theory of deep learning," *Journal of Statistical Mechanics: Theory and Experiment*, vol. 2019, no. 12, p. 124020, 2019.
- [15] R. Shwartz-Ziv and N. Tishby, "Opening the black box of deep neural networks via information," arXiv preprint arXiv:1703.00810, 2017.

- [16] N. Tishby, F. C. Pereira, and W. Bialek, "The information bottleneck method," arXiv preprint physics/0004057, 2000.
- [17] Z. Goldfeld, E. Van Den Berg, K. Greenewald, I. Melnyk, N. Nguyen, B. Kingsbury, and Y. Polyanskiy, "Estimating information flow in deep neural networks," in *International Conference on Machine Learning*, 2019, pp. 2299–2308.
- [18] M. D. Zeiler and R. Fergus, "Visualizing and understanding convolutional networks," in *European Conference on Computer Vision*. Springer, 2014, pp. 818–833.
- [19] A. Mahendran and A. Vedaldi, "Understanding deep image representations by inverting them," in *Proceedings of the IEEE Conference on Computer Vision and Pattern Recogni*tion, 2015, pp. 5188–5196.
- [20] J. Yosinski, J. Clune, A. Nguyen, T. Fuchs, and H. Lipson, "Understanding neural networks through deep visualization," arXiv preprint arXiv:1506.06579, 2015.
- [21] R. Shokri and V. Shmatikov, "Privacy-preserving deep learning," in *Proceedings of the 22nd ACM SIGSAC conference* on computer and communications security, 2015, pp. 1310– 1321.
- [22] H. B. McMahan, G. Andrew, U. Erlingsson, S. Chien, I. Mironov, N. Papernot, and P. Kairouz, "A general approach to adding differential privacy to iterative training procedures," arXiv preprint arXiv:1812.06210, 2018.
- [23] F. Mo, A. S. Shamsabadi, K. Katevas, S. Demetriou, I. Leontiadis, A. Cavallaro, and H. Haddadi, "DarkneTZ: towards model privacy at the edge using trusted execution environments," in *Proceedings of the 18th International* Conference on Mobile Systems, Applications, and Services, 2020, pp. 161–174.
- [24] F. Mo, H. Hamed, K. Katevas, E. Marin, D. Perino, and N. Kourtellis, "PPFL: Privacy-preserving federated learning with trusted execution environments," in *Proceedings of the* 19th International Conference on Mobile Systems, Applications, and Services, 2021.
- [25] Z. Gu, H. Huang, J. Zhang, D. Su, H. Jamjoom, A. Lamba, D. Pendarakis, and I. Molloy, "Yerbabuena: Securing deep learning inference data via enclave-based ternary model partitioning," arXiv preprint arXiv:1807.00969, 2018.
- [26] Y. Xu, S. Zhao, J. Song, R. Stewart, and S. Ermon, "A theory of usable information under computational constraints," in *International Conference on Learning Representations* (ICLR), 2020.
- [27] P. Kairouz, H. B. McMahan, B. Avent, A. Bellet, M. Bennis, A. N. Bhagoji, K. Bonawitz, Z. Charles, G. Cormode, R. Cummings et al., "Advances and open problems in federated learning," arXiv preprint arXiv:1912.04977, 2019.
- [28] K. Ganju, Q. Wang, W. Yang, C. A. Gunter, and N. Borisov, "Property inference attacks on fully connected neural networks using permutation invariant representations," in Proceedings of the 2018 ACM SIGSAC Conference on Computer and Communications Security, 2018, pp. 619–633.
- [29] R. Shokri, M. Stronati, C. Song, and V. Shmatikov, "Membership inference attacks against machine learning models," in 2017 IEEE Symposium on Security and Privacy (SP). IEEE, 2017, pp. 3–18.
- [30] J. Zhu and M. Blaschko, "R-gap: Recursive gradient attack on privacy," arXiv preprint arXiv:2010.07733, 2020.
- [31] L. Fan, K. W. Ng, C. Ju, T. Zhang, C. Liu, C. S. Chan, and Q. Yang, "Rethinking privacy preserving deep learning:

- How to evaluate and thwart privacy attacks," in *Federated Learning*. Springer, 2020, pp. 32–50.
- [32] Y. Aono, T. Hayashi, L. Wang, S. Moriai et al., "Privacy-preserving deep learning via additively homomorphic encryption," *IEEE Transactions on Information Forensics and Security*, vol. 13, no. 5, pp. 1333–1345, 2017.
- [33] A. D. Wyner, "The wire-tap channel," Bell system technical journal, vol. 54, no. 8, pp. 1355–1387, 1975.
- [34] G. Montavon, K.-R. Müller, and M. Braun, "Layer-wise analysis of deep networks with Gaussian kernels," Advances in Neural Information Processing Systems, vol. 23, pp. 1678– 1686, 2010.
- [35] A. Choromanska, M. Henaff, M. Mathieu, G. B. Arous, and Y. LeCun, "The loss surfaces of multilayer networks," in Artificial Intelligence and Statistics. PMLR, 2015, pp. 192–204.
- [36] L. Huang, J. Qin, L. Liu, F. Zhu, and L. Shao, "Layer-wise conditioning analysis in exploring the learning dynamics of dnns," in *European Conference on Computer Vision*. Springer, 2020, pp. 384–401.
- [37] C. E. Shannon, "A mathematical theory of communication," The Bell system technical journal, vol. 27, no. 3, pp. 379– 423, 1948.
- [38] ——, "Communication theory of secrecy systems," The Bell system technical journal, vol. 28, no. 4, pp. 656–715, 1949.
- [39] M. I. Belghazi, A. Baratin, S. Rajeshwar, S. Ozair, Y. Bengio, A. Courville, and D. Hjelm, "Mutual information neural estimation," in *International Conference on Machine Learning*, 2018, pp. 531–540.
- [40] Y. LeCun, L. Bottou, Y. Bengio, and P. Haffner, "Gradient-based learning applied to document recognition," *Proceedings of the IEEE*, vol. 86, no. 11, pp. 2278–2324, 1998.
- [41] A. Sablayrolles, M. Douze, C. Schmid, Y. Ollivier, and H. Jégou, "White-box vs black-box: Bayes optimal strategies for membership inference," in *International Conference* on *Machine Learning*, 2019, pp. 5558–5567.
- [42] C. M. Bishop, "Pattern recognition," Machine learning, vol. 128, no. 9, 2006.
- [43] Z. Wang, A. C. Bovik, H. R. Sheikh, and E. P. Simoncelli, "Image quality assessment: from error visibility to structural similarity," *IEEE Transactions on Image Processing*, vol. 13, no. 4, pp. 600–612, 2004.
- [44] F. Draxler, K. Veschgini, M. Salmhofer, and F. Hamprecht, "Essentially no barriers in neural network energy landscape," in *International conference on machine learning*. PMLR, 2018, pp. 1309–1318.
- [45] T. Zahavy, B. Kang, A. Sivak, J. Feng, H. Xu, and S. Mannor, "Ensemble robustness and generalization of stochastic deep learning algorithms," in *International Conference on Learning Representations Workshop*, 2018.
- [46] G. W. Ding, K. Y. C. Lui, X. Jin, L. Wang, and R. Huang, "On the sensitivity of adversarial robustness to input data distributions," in *International Conference on Learning Rep*resentations, 2018.
- [47] M. Lecuyer, V. Atlidakis, R. Geambasu, D. Hsu, and S. Jana, "Certified robustness to adversarial examples with differential privacy," in 2019 IEEE Symposium on Security and Privacy (SP). IEEE, 2019, pp. 656–672.
- [48] R. Novak, Y. Bahri, D. A. Abolafia, J. Pennington, and J. Sohl-Dickstein, "Sensitivity and generalization in neural

- networks: an empirical study," in *International Conference on Learning Representations (ICLR)*, 2018.
- [49] J. Sokolić, R. Giryes, G. Sapiro, and M. R. Rodrigues, "Robust large margin deep neural networks," *IEEE Transactions* on Signal Processing, vol. 65, no. 16, pp. 4265–4280, 2017.
- [50] M. Cissé, P. Bojanowski, E. Grave, Y. Dauphin, and N. Usunier, "Parseval networks: Improving robustness to adversarial examples," in *International Conference on Machine Learning*, 2017.
- [51] Z. Drmac, "On principal angles between subspaces of Euclidean space," SIAM Journal on Matrix Analysis and Applications, vol. 22, no. 1, pp. 173–194, 2000.
- [52] K. Ye and L.-H. Lim, "Schubert varieties and distances between subspaces of different dimensions," SIAM Journal on Matrix Analysis and Applications, vol. 37, no. 3, pp. 1176–1197, 2016.
- [53] A. Björck and G. H. Golub, "Numerical methods for computing angles between linear subspaces," *Mathematics of Computation*, vol. 27, no. 123, pp. 579–594, 1973.
- [54] A. Krizhevsky et al., "Learning multiple layers of features from tiny images," Citeseer, 2009.
- [55] G. B. Huang, M. Mattar, T. Berg, and E. Learned-Miller, "Labeled faces in the wild: A database for studying face recognition in unconstrained environments," in Workshop on faces in'Real-Life'Images: detection, alignment, and recognition. 2008.
- [56] Z. Liu, P. Luo, X. Wang, and X. Tang, "Deep learning face attributes in the wild," in *Proceedings of International Con*ference on Computer Vision (ICCV), December 2015.
- [57] N. Kumar, A. C. Berg, P. N. Belhumeur, and S. K. Nayar, "Attribute and simile classifiers for face verification," in 2009 IEEE 12th International Conference on Computer Vision. IEEE, 2009, pp. 365–372.
- [58] A. Maas, R. E. Daly, P. T. Pham, D. Huang, A. Y. Ng, and C. Potts, "Learning word vectors for sentiment analysis," in Proceedings of the 49th annual meeting of the association for computational linguistics: Human language technologies, 2011, pp. 142–150.
- [59] B. Verhoeven and W. Daelemans, "CLiPS Stylometry Investigation (CSI) corpus: A Dutch corpus for the detection of age, gender, personality, sentiment and deception in text," in *LREC*, 2014, pp. 3081–3085.
- [60] N. Pinto, Z. Stone, T. Zickler, and D. Cox, "Scaling up biologically-inspired computer vision: A case study in unconstrained face recognition on facebook," in CVPR 2011 WORKSHOPS. IEEE, 2011, pp. 35–42.
- [61] W. S. Cleveland and S. J. Devlin, "Locally weighted regression: an approach to regression analysis by local fitting," Journal of the American Statistical Association, vol. 83, no. 403, pp. 596–610, 1988.
- [62] A. Wainakh, F. Ventola, T. Müßig, J. Keim, C. G. Cordero, E. Zimmer, T. Grube, K. Kersting, and M. Mühlhäuser, "User label leakage from gradients in federated learning," arXiv preprint arXiv:2105.09369, 2021.
- [63] B. Jayaraman and D. Evans, "Evaluating differentially private machine learning in practice," in 28th {USENIX} Security Symposium, 2019, pp. 1895–1912.
- [64] H. Wang, M. Yurochkin, Y. Sun, D. Papailiopoulos, and Y. Khazaeni, "Federated learning with matched averaging," in *International Conference on Learning Representations*,

2019.

- [65] V. Pichapati, A. T. Suresh, F. X. Yu, S. J. Reddi, and S. Kumar, "Adaclip: Adaptive clipping for private sgd," arXiv preprint arXiv:1908.07643, 2019.
- [66] K. He, X. Zhang, S. Ren, and J. Sun, "Deep residual learning for image recognition," in *Proceedings of the IEEE Conference on Computer Vision and Pattern Recognition*, 2016, pp. 770–778.
- [67] A. Sherstinsky, "Fundamentals of recurrent neural network (rnn) and long short-term memory (lstm) network," *Physica D: Nonlinear Phenomena*, vol. 404, p. 132306, 2020.
- [68] Z. Wu, S. Pan, F. Chen, G. Long, C. Zhang, and S. Y. Philip, "A comprehensive survey on graph neural networks," *IEEE transactions on neural networks and learning systems*, 2020.
- [69] A. G. Wilson and P. Izmailov, "Bayesian deep learning and a probabilistic perspective of generalization," Advances in Neural Information Processing Systems, 2020.